IOSR Journal of Applied Physics (IOSR-JAP)
e-ISSN: 2278-4861.Volume 17, Issue 2 Ser. 1 (Mar. – Apr. 2025), PP 28-33
www.iosrjournals.org

Spectral and Photoluminescence Properties of Nd^{3+} Doped Borotellurite Glasses for 1.08 µm photonic devices

S.L.Meena
Ceramic Laboratory, Department of physics, Jai Narain Vyas University, Jodhpur 342001(Raj.) India
E-mail address:shankardiya7@rediffmail.com

Abstract
Glass of the system :(40-x)TeO_2:10ZnO:10Li_2O:10Na_2O:10WO_3:20B_2O_3:xNd_2O_3. (where x=1, 1.5,2 mol %) have been prepared by melt-quenching method. The amorphous nature of the glasses was confirmed by X-ray diffraction studies. Optical absorption spectra were recorded at room temperature for all glass samples. Slater-Condon parameters F_k (k=2, 4, 6), Lande parameter ξ_{4f} and Racah parameters E^k (k=1, 2, 3) have been computed. Using these parameters energies and intensities of these bands has been calculated. Judd-Ofelt intensity parameters Ω_λ (λ=2, 4, 6) are evaluated from the intensities of various absorption bands of optical absorption spectra. Using these intensity parameters various radiative properties like spontaneous emission probability (A), branching ratio (β_R), radiative life time (τ_R) and stimulated emission cross–section (σ_p)) of various emission lines have been evaluated.

Keywords: *ZLSTBT Glasses, Optical Properties, Judd-Ofelt Theory, Photoluminescence Properties.*

Date of Submission: 05-03-2025 Date of Acceptance: 17-03-2025

I. Introduction

Among different ceramic glasses, scientific interest on borotellurite glasses is attributed to their favorable properties such as, high density, high refractive index, large third order nonlinear optical susceptibility [1-6].Tellurite glass is an extremely promising material for reflecting windows, laser, mechanical sensors and nonlinear applications in optics due to some of its essential characteristic features, such as low phonon energy, low melting temperature and excellent transparency. They have high thermal stability, high transparency and low dispersion rates [7-12].

Tellurite glasses are potentially important host materials for developing rare earth doped optical devices. Tellurite glasses have excellent transparency, good mechanical and thermal stability. Borotellurite glass has low phonon energy, chemical and thermal stability [13,14]. Thus, it can be widely used in visible and infrared laser, fiber amplifier and optical data storage devices. They present superior properties like that high transparency, low melting point, high gain density, high solubility for rare-earth ions and low dispersion. The host matrix compose of ZnO, a glass modifier/glass farmer a heavy metal oxide along with TeO_2, Li_2O, Na_2O, WO_3 and B_2O_3.The addition of Na_2O to the glass mixture improves the rare earth ion solubility leading to the possibility of using even higher concentrations of ions [15-18].

The present work reports on the absorption and emission properties of Nd^{3+} doped zinc lithium sodium tungsten borotellurite glass. The intensities of the transitions for the rare earth ions have been estimated successfully using the Judd-Ofelt theory, The laser parameters such as radiative probabilities (A), branching ratio (β_R), radiative life time (τ_R) and stimulated emission cross section(σ_p) are evaluated using J.O. intensity parameters (Ω_λ, λ=2,4 and 6).

II. Experimental Techniques

Preparation of glasses

The following Nd^{3+} doped borotellurite glass samples :(40-x)TeO_2:10ZnO:10Li_2O:10Na_2O:10WO_3:20B_2O_3: xNd_2O_3. (where *x* =1, 1.5, 2) have been prepared by melt-quenching method. Analytical reagent grade chemical used in the present study consist of TeO_2, ZnO, Li_2O, Na_2O, WO_3, B_2O_3 and Nd_2O_3. They were thoroughly mixed by using an agate pestle mortar. Then melted at 975˚C by an electrical muffle furnace for 2 hours. After complete melting, the melts were quickly poured in to a preheated stainless steel mould and annealed at temperature of 250˚C for 2 h to remove thermal strains and stresses. Every time fine powder of cerium oxide was used for polishing the samples. The glass samples so prepared were of good optical quality and were transparent. The chemical compositions of the glasses with the name of samples are summarized in **Table 1.**

Table 1.

Sample	Glass composition (mol %)
ZLSTBT (UD)	$40TeO_2:10ZnO:10Li_2O:10Na_2O:10WO_3:20B_2O_3$
ZLSTBT (ND1)	$39TeO_2:10ZnO:10Li_2O:10Na_2O:10WO_3:20B_2O_3:1Nd_2O_3$
ZLSTBT (ND1.5)	$38.5TeO_2:10ZnO:10Li_2O:10Na_2O:10WO_3:20B_2O_3:1.5Nd_2O_3$
ZLSTBT (ND2)	$38TeO_2:10ZnO:10Li_2O:10Na_2O:10WO_3:20B_2O_3: 2Nd_2O_3$

ZLSTBT (UD) - Represents undoped Zinc Lithium Sodium Tungsten Borotellurite glass specimen.
ZLSTBT (ND) - Represents Nd^{3+} doped Zinc Lithium Sodium Tungsten Borotellurite glass specimens.

III. Theory

3.1 Oscillator Strength

The intensity of spectral lines is expressed in terms of oscillator strengths using the relation [19].

$$f_{expt.} = 4.318 \times 10^{-9} \int \varepsilon (\nu)\, d\nu \qquad (1)$$

where, $\varepsilon (\nu)$ is molar absorption coefficient at a given energy ν (cm^{-1}), to be evaluated from Beer–Lambert law. Under Gaussian Approximation, using Beer–Lambert law, the observed oscillator strengths of the absorption bands have been experimentally calculated [20], using the modified relation:

$$P_m = 4.6 \times 10^{-9} \times \frac{1}{cl} \log \frac{I_0}{I} \times \Delta\upsilon_{1/2} \qquad (2)$$

Where c is the molar concentration of the absorbing ion per unit volume, I is the optical path length, $\log I_0/I$ is optical density and $\Delta\upsilon_{1/2}$ is half band width.

3.2. Judd-Ofelt Intensity Parameters

According to Judd [21] and Ofelt [22] theory, independently derived expression for the oscillator strength of the induced forced electric dipole transitions between an initial J manifold $|4f^N (S, L) J\rangle$ level and the terminal J' manifold $|4f^N (S', L') J'\rangle$ is given by:

$$\frac{8\Pi^2 mc\bar{\upsilon}}{3h(2J+1)} \frac{1}{n} \left[\frac{(n^2+2)^2}{9} \right] \times S(J, J') \qquad (3)$$

Where, the line strength S (J, J') is given by the equation

$$S(J, J') = e^2 \sum_{\lambda = 2, 4, 6} \Omega_\lambda \langle 4f^N (S, L) J \| U^{(\lambda)} \| 4f^N (S', L') J' \rangle 2 \qquad (4)$$

In the above equation m is the mass of an electron, c is the velocity of light, ν is the wave number of the transition, h is Planck's constant, n is the refractive index, J and J' are the total angular momentum of the initial and final level respectively, Ω_λ (λ=2,4and 6) are known as Judd-Ofelt intensity parameters.

3.3 Radiative Properties

The Ω_λ parameters obtained using the absorption spectral results have been used to predict radiative properties such as spontaneous emission probability (A) and radiative life time (τ_R), and laser parameters like fluorescence branching ratio (β_R) and stimulated emission cross section (σ_p).

The spontaneous emission probability from initial manifold $|4f^N (S', L') J'\rangle$ to a final manifold $|4f^N (S, L) J\rangle|$ is given by:

$$A[(S', L') J'; (S, L) J] = \frac{64\pi^2\nu^3}{3h(2J'+1)} \left[\frac{n(n^2+2)^2}{9} \right] \times S(J', \bar{J}) \qquad (5)$$

Where, $S(J', J) = e^2 [\Omega_2 \| U^{(2)} \|^2 + \Omega_4 \| U^{(4)} \|^2 + \Omega_6 \| U^{(6)} \|^2]$

The fluorescence branching ratio for the transitions originating from a specific initial manifold $|4f^N (S', L') J'\rangle$ to a final many fold $|4f^N (S, L) J\rangle$ is given by

$$\beta [(S', L') J'; (S, L) J] = \sum_{SLJ} \frac{A[(S' L)]}{A[(S' L') J'(\bar{S} L)]} \quad (6)$$

The radiative life time is given by

$$\tau_{rad} = \sum_{SLJ} A[(S', L') J'; (S,L)] = A_{Total}^{-1} \quad (7)$$

Where, the sum is over all possible terminal manifolds. The stimulated emission cross -section for a transition from an initial manifold $|4f^N (S', L') J'\rangle$ to a final manifold $|4f^N (S, L) J\rangle$ is expressed as

$$\sigma_p(\lambda_p) = \left[\frac{\lambda_p^4}{8\pi c n^2 \Delta\lambda_{eff}}\right] \times A[(S', L') J'; (\bar{S}, \bar{L})\bar{J}] \quad (8)$$

Where, λ_p the peak fluorescence wavelength of the emission band and $\Delta\lambda_{eff}$ is the effective fluorescence line width.

3.4 Nephelauxetic Ratio (β) and Bonding Parameter ($b^{1/2}$)

The nature of the R-O bond is known by the Nephelauxetic Ratio (β') and Bonding Parameters ($b^{1/2}$), which are computed by using following formulae [23,24]. The Nephelauxetic Ratio is given by

$$\beta' = \frac{\nu_g}{\nu_a} \quad (9)$$

where, ν_a and ν_g refer to the energies of the corresponding transition in the glass and free ion, respectively. The values of bonding parameter $b^{1/2}$ are given by

$$b^{1/2} = \left[\frac{1-\beta'}{2}\right]^{1/2} \quad (10)$$

IV. Result and Discussion

4.1. XRD Measurement

Figure 1 presents the XRD pattern of the samples shows no sharp Bragg's peak, but only a broad diffuse hump around low angle region. This is the clear indication of amorphous nature within the resolution limit of XRD instrument.

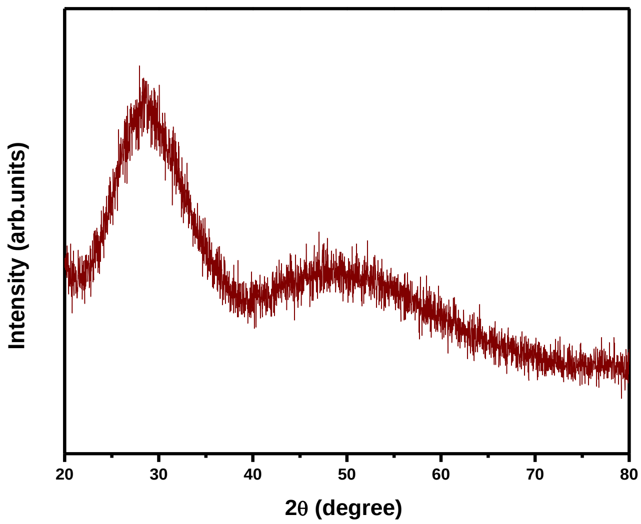

Fig.1: X-ray diffraction pattern of ZLSTBT (ND 01) glass.

4.2. Absorption spectra

The absorption spectra of ZLSTBT (ND01) glass, consists of absorption bands corresponding to the absorptions from the ground state $^4I_{9/2}$ of Nd^{3+} ions. Nine absorption bands have been observed from the ground state $^4I_{9/2}$ to excited states $^4F_{3/2}$, $^4F_{5/2}$, $^4F_{7/2}$, $^4F_{9/2}$, $^2H_{11/2}$, $^4G_{5/2}$, $^4G_{7/2}$, $^4G_{9/2}$, and $^2G_{9/2}$ for Nd^{3+} doped ZLSTBT (ND 01) glass.

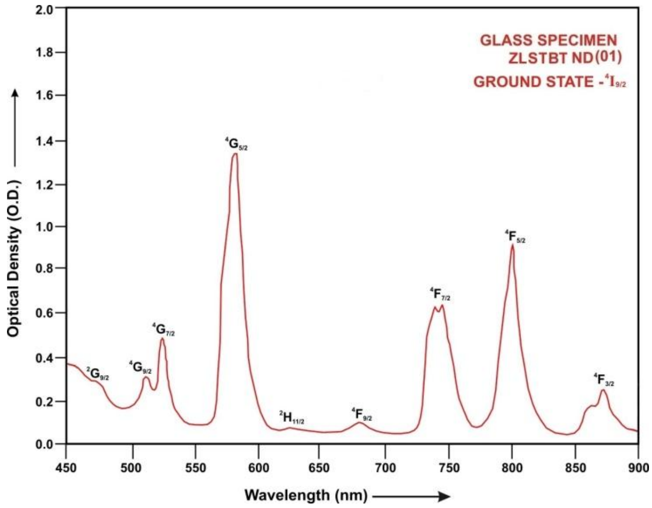

Fig.2: Absorption spectra of ZLSTBT (ND 01) glass.

The experimental and calculated oscillator strength for Nd^{3+} ions in ZLSTBT glasses are given in **Table 2.**

Table 2. Measured and calculated oscillator strength ($P^m \times 10^{+6}$) of Nd^{3+} ions in ZLSTBT glasses.

Energy level from $^4I_{9/2}$	Glass ZLSTBT (ND01)		Glass ZLSTBT (ND1.5)		Glass ZLSTBT (ND02)	
	$P_{exp.}$	$P_{cal.}$	$P_{exp.}$	$P_{cal.}$	$P_{exp.}$	$P_{cal.}$
$^4F_{3/2}$	3.47	3.66	3.42	3.65	3.37	3.63
$^4F_{5/2}$	8.75	8.59	8.71	8.55	8.63	8.50
$^4F_{7/2}$	9.35	9.87	9.28	9.82	9.23	9.79
$^4F_{9/2}$	0.65	0.53	0.63	0.53	0.60	0.52
$^2H_{11/2}$	0.25	0.15	0.22	0.15	0.20	0.15
$^4G_{5/2}$	25.75	26.10	24.65	25.03	23.56	23.96
$^4G_{7/2}$	4.25	5.24	4.20	5.16	4.15	5.08
$^4G_{9/2}$	2.26	2.28	2.21	2.26	2.16	2.25
$^2G_{9/2}$	0.94	2.90	0.92	2.89	0.89	2.88
r.m.s.deviation	0.7681		0.7718		0.7735	

Table3. Computed values of Slater-Condon, Lande, Racah, nephelauexetic ratio and bonding parameter for Nd^{3+} doped ZLSTBT glass specimens.

Parameter	Free ion	ZLSTBT (ND01)	ZLSTBT (ND1.5)	ZLSTBT (ND02)
$F_2(cm^{-1})$	331.16	324.58	324.64	324.65
$F_4(cm^{-1})$	50.71	50.72	50.72	50.72
$F_6(cm^{-1})$	5.154	5.038	5.041	5.042
$\xi_{4f}(cm^{-1})$	884.0	882.73	882.67	882.66
$E^1(cm^{-1})$	5024.0	4947.12	4948.19	494.83
$E^2(cm^{-1})$	23.90	23.08	23.09	23.09
$E^3(cm^{-1})$	497.0	489.58	489.58	489.59
F_4/F_2	0.1531	0.1563	0.1562	0.1562
F_6/F_2	0.0155	0.0155	0.0155	0.0155
E^1/E^3	10.1086	10.1048	10.1070	10.1069
E^2/E^3	0.0481	0.0471	0.0472	0.0472
β'		0.9958	0.9960	0.9961
$b^{1/2}$		0.04578	0.04449	0.04444

The values of Judd-Ofelt intensity parameters are given in **Table 4**.

Table 4. Judd-Ofelt intensity parameters for Nd^{3+} doped ZLSTBT glass specimens.

Glass Specimen	Ω_2(pm^2)	Ω_4(pm^2)	Ω_6(pm^2)	Ω_4/Ω_6
ZLSTBT (ND01)	2.716	7.744	3.559	2.176
ZLSTBT (ND1.5)	2.361	7.724	3.541	2.181
ZLSTBT (ND02)	2.032	7.671	3.528	2.174

4.3. Excitation Spectrum

The Excitation spectra of Nd^{3+}doped ZLSTBT ND (01) glass specimen has been presented in Figure 3 in terms of Excitation Intensity versus wavelength. The excitation spectrum was recorded in the spectral region 700–1000 nm fluorescence at 1065nm having different excitation band centred at 808 nm and 887 nm are attributed to the ($^4I_{9/2}\rightarrow{}^4F_{5/2}$) and ($^4I_{9/2}\rightarrow{}^4F_{3/2}$) transitions, respectively. The highest absorption level is ($^4I_{9/2}\rightarrow{}^4F_{5/2}$) and is at 808 nm. So this is to be chosen for excitation wavelength.

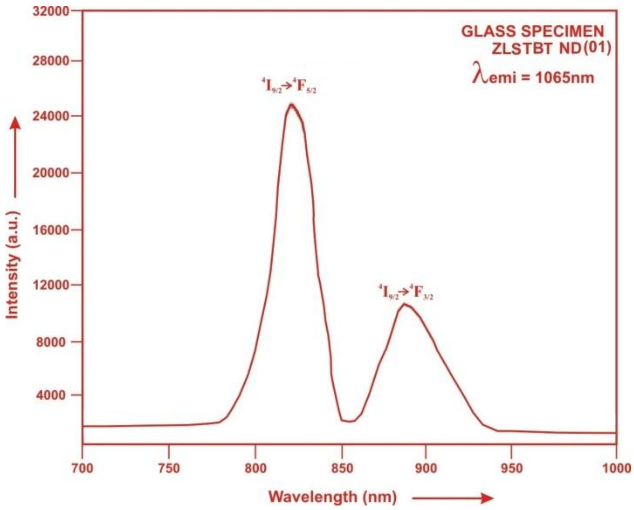

Fig.3: Excitation spectra of ZLSTBT (ND 01) glass.

4.4. Fluorescence Spectrum

The fluorescence spectrum of Nd^{3+}doped in zinc lithium sodium tungsten borotellurite is shown in Figure 4. There are six broad bands ($^4G_{7/2}\rightarrow{}^4I_{9/2}$), ($^4G_{7/2}\rightarrow{}^4I_{11/2}$), ($^4F_{3/2}\rightarrow{}^4I_{9/2}$) ($^4F_{3/2}\rightarrow{}^4I_{11/2}$), ($^4F_{3/2}\rightarrow{}^4I_{13/2}$) and ($^4F_{3/2}\rightarrow{}^4I_{15/2}$) respectively for glass specimens.

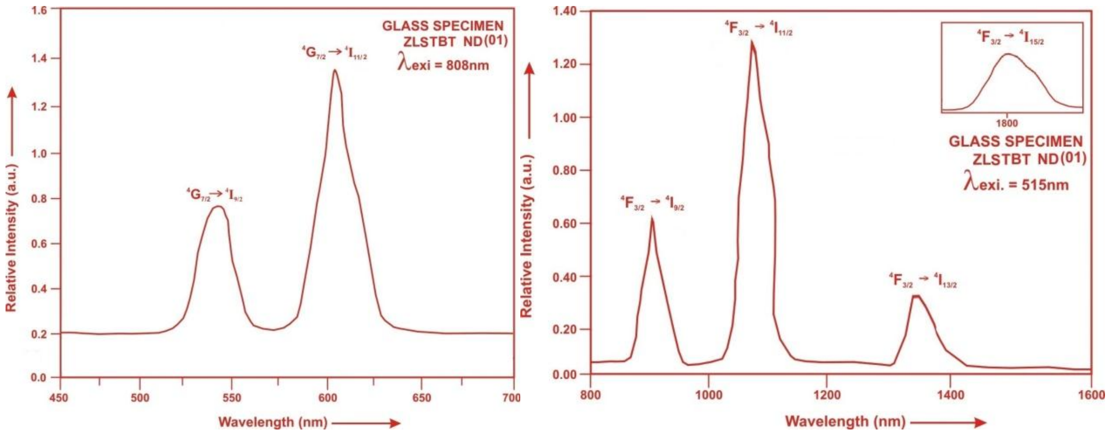

Fig.4: Fluorescence spectrum of ZLSTBT glasses doped with Nd^{3+}.

The wavelengths of these bands along with their assignments are given in **Table 5**.

Table 5. Emission peak wave lengths (λ_p), radiative transition probability (A_{rad}), branching ratio (β_R), stimulated emission crosssection (σ_p), and radiative life time (τ_R) for various transitions in Nd^{3+} doped ZLSTBT glasses.

Transition		ZLSTBT (ND 01)				ZLSTBT (ND 1.5)				ZLSTBT (ND 02)			
	λ_{max} (nm)	$A_{rad}(s^{-1})$	β	σ_p (10^{-20} cm^2)	τ_R(µs)	$A_{rad}(s^{-1})$	β	σ_p (10^{-20} cm^2)	τ_R (µs)	$A_{rad}(s^{-1})$	β	σ_p (10^{-20} cm^2)	τ_R (10^{-20} cm^2)
$^4G_{7/2}\rightarrow{}^4I_{9/2}$	532	3159.17	0.4195	0.483		3108.83	0.4249	0.496		3051.05	0.4301	0.5086	
$^4G_{7/2}\rightarrow{}^4I_{11/2}$	595	3058.93	0.4062	1.190		2896.47	0.3959	1.243		2737.41	0.3858	1.243	
$^4F_{3/2}\rightarrow{}^4I_{9/2}$	905	779.32	0.1035	0.767		778.68	0.1064	0.780		775.13	0.1093	0.805	
$^4F_{3/2}\rightarrow{}^4I_{11/2}$	1075	456.90	0.0607	2.152	132.78	456.00	0.0623	2.444	136.68	454.59	0.0641	2.516	140.95
$^4F_{3/2}\rightarrow{}^4I_{13/2}$	1320	74.90	0.0099	0.432		74.67	0.0102	0.451		74.55	0.0105	0.471	
$^4F_{3/2}\rightarrow{}^4I_{15/2}$	1800	1.79	0.0002	0.026		1.78	0.0002	0.026		1.78	0.0003	0.027	

V. Conclusion

In the present study, the glass samples of composition :(40-x)TeO_2:10ZnO:10Li_2O:10Na_2O:10WO_3:20B_2O_3: xNd_2O_3. (where x =1, 1.5, 2 mol %) have been prepared by melt-quenching method. The stimulated emission cross section (σ_p) has highest value for the transition ($^4F_{3/2}\rightarrow{}^4I_{11/2}$) in all the glass specimens doped with Nd^{3+} ion. This shows that ($^4F_{3/2}\rightarrow{}^4I_{11/2}$) transition is most probable transition. The results show that the Nd^{3+} doped borotellurite glasses could be potential candidates for 1.08 µm photonic devices.

References

[1]. Xia,Y.J.,Zhang,T.(2024).Advances in the optical and electronic properties and applications of bismuth based semiconductor materials.J.Mat.Chem. C 12,1609-1624.

[2]. Meena,S.L.(2023).Spectral and Raman analysis of Er^{3+} doped ytterbium zinc lithium sodalime magnesium borophosphate glasses,Int.Inn.Res.Sci.Eng.Tech.12,10915-24.

[3]. Kaur, R.B.R., Kumar,A.(2021).Physical,optical,structural and thermoluminescence behavior of borosilicate glass doped with trivalent neodymium ions,Opt.Mat.117,1-13

[4]. Matous,I.S.,Balzaretti,N.M.(2024).Effect of mixed alkali ions on the structural and spectroscopic properties of Nd^{3+} doped silicate glasses,Results Mat.21,100517.

[5]. Asyikin,A.S.,Halimah,M.K.,Latif,A.A.,Faznny,M.F.,Nazrin,S.N.(2020).Physical,structural and optical properties of bio-silica borotellurite glass system doped with samarium oxide nanoparticles,J.Non-Cryst.Solids,529,119777.

[6]. Reddy,K.S.R.K.,Swapna,K.,Mahamuda,Sk.,Venkateswarulu,M.,Rao,A.S.(2021).Structural,optical and photoluminescence properties of alkaline-earth borotellurite glass doped with trivalent Neodymium for 1.06 µm optoelectronic devices

[7]. Laxmikanth,C., Elias,A.M., Sichone,S., Mwankemwa(2025).Tailoring structural, thermal and optical properties of Tm^{3+} doped borotellurite glass through Bi_2O_3 incorporation for optical fiber construction,Next Mat.6,100274

[8]. Klimesz,B.,Romanowski,W.R.,Lisiecki,R.(2024)Spectroscopic and Thermographic qualities of praseodymium doped oxyfluorotellurite glasses,Molecules,29,3041.

[9]. Elias,A.M.,Mwanga,S.F.,Mwankemwa,B.,Anjaiah,J.,Laxmikanth,C.(2022).Influence of Bi^+ ions on photoluminescence properties of Tm_2O_3 doped borotellurite glasses for the near-infrared emission applications,Opt.Mat.125,112140.

[10]. Sayyed, M.I.,AL-Hadeethi, Y., Alshammari, M.M., Ahmed,M., AlHeniti, S.H., Rammah,Y.S.(202).Physical,optical and gamma radiation shielding competence of newly borotellurite based glasses:TeO_2-B_2O_3-ZnO-Li_2O_3-Bi_2O_3,Ceram.Int. 47,611-618

[11]. Kashif,I.,Ratep,A.(2023).Influence of dysprosium oxide on physical and optical characteristics of zinc boro-tellurite glasses for optoelectronic device application,Res.Opt.11,100401.

[12]. Gomes,J.F.,Lima,A.M.O.,Sandrini,M.,Medina,A.N.,Steimacher,A.,Pedrochi,F.,Barboza,M.J.(2017).Optical and spectroscopic study of erbium doped calcium borotellurite glasses,Opt.Mat.66,211-219.

[13]. Gowda, G.V.J., Reddy,G.V.A., Eraiah,B., Devaraja, C.R.(2023).Investigation of structural modification, physical and optical properties of lead boro-tellurite glasses doped with europium trioxide for possible optical switching applications.J.Met.Min.33,65-74

[14]. Meena,S.L.(2024).Spectral, Thermal and Upconversion properties of Dy^{3+} doped borotellurite glasses with large stability parameter, IOSR Appl.Phys.42-49.

[15]. Anjaiah,J., Laxmikanth,C.(2015). Optical Properties of Neodymium Ion Doped Lithium Borate Glasses, 5,173 -183.

[16]. Devi,R.,Jayasankar,C.K.(1995). Optical properties of Nd^{3+} ions in lithium borate glasses, Mat. Chem. Phys, 42,106-119.

[17]. Pal, M., Roy, B.and Pal, M. (2011). Structural characterization of borate glasses containing zinc and manganese oxide. J.Mod.Physics, 2, 1062-66.

[18]. Weber, M.J. (1990). Science and technology of laser glass. J. Non-Cryst. Solids, 123, 208–222.

[19]. Meena,S.L.(2024).Spectral and Thermal analysis of praseodymium doped bismuth borate glasses for thermionic applications.IOSR Appl.Phys.16,20-27.

[20]. Meena,S.L.(2022).Spectral and Upconversion properties of Dy^{3+} ions doped zinc lithium potessiumniobate borosilicate glasses,Int.J.Eng.Sci.Inv.11,44-49.

[21]. Judd, B.R.(1962).Optical absorption intensities of rare earth ions,Phys.Rev.127,750 761.

[22]. Ofelt,G.S. (1962). Intensities of crystal spectra of rare earth Ions, Chem.Phys37, 511-520.

[23]. Sinha, S.P. (1983). Systematics and properties of lanthanides, Reidel, Dordrecht.

[24]. Krupke, W.F. (1974).IEEE J. Quantum Electron QE, 10,450